# SPARC: Spatio-Temporal Adaptive Resource Control for Multi-site Spectrum Management in NextG Cellular Networks

# ANONYMOUS AUTHOR(S)

This work presents SPARC (Spatio-Temporal Adaptive Resource Control), a novel approach for multi-site spectrum management in NextG cellular networks. SPARC addresses the challenge of limited licensed spectrum in dynamic environments. We leverage the O-RAN architecture to develop a multi-timescale RAN Intelligent Controller (RIC) framework, featuring an xApp for near-real-time interference detection and localization, and a  $\mu$ App for real-time intelligent resource allocation. By utilizing base stations as spectrum sensors, SPARC enables efficient and fine-grained dynamic resource allocation across multiple sites, enhancing signal-to-noise ratio (SNR) by up to 7dB, spectral efficiency by up to 15%, and overall system throughput by up to 20%. Comprehensive evaluations, including emulations and over-the-air experiments, demonstrate the significant performance gains achieved through SPARC, showcasing it as a promising solution for optimizing resource efficiency and network performance in NextG cellular networks.

#### 1 INTRODUCTION

The rapid growth of next-generation applications places substantial demands on data throughput, latency, and reliability in modern communication networks. These applications increasingly rely on 5G technology to connect them to cloud and edge computing services, extending beyond traditional wide area networks to private 5G networks designed for enclosed spaces such as large enterprises, warehouses and office buildings. Network-sensitive applications like industrial IoT, which demand high reliability, and AR/VR, which are extremely data-intensive and require low latency, further emphasize the need for advanced network management solutions.

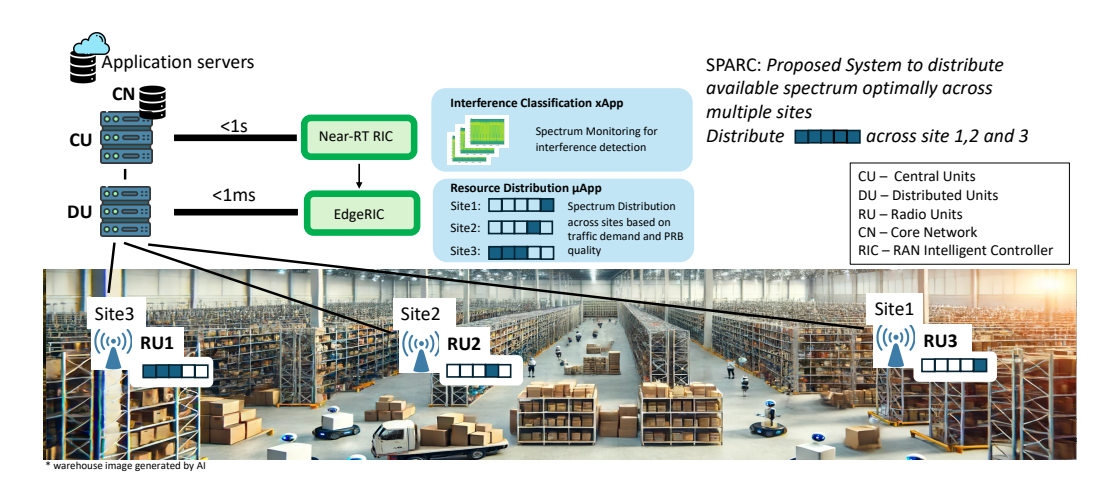


Fig. 1. System and Network Overview

A critical challenge in these deployments is the limited availability of licensed spectrum, necessitating efficient frequency reuse strategies across cell sites that jointly provide coverage over the space as shown in Figure 1. Here, three cell sites jointly provide coverage over a limited area and spectrum resources must be allocated across them. This paper introduces SPARC (Spatio-Temporal Adaptive Resource Control), a novel approach for multi-site spectrum management in NextG cellular networks. SPARC addresses the challenge of limited licensed spectrum in dynamic environments

:2 Anon.

by leveraging the Open Radio Access Network (O-RAN) architecture that enables monitoring and control of radio access networks at different timescales.

Our approach centers on developing a multi-timescale RAN Intelligent Controller (RIC) framework, featuring an xApp for near-real-time (< 1s) interference detection and localization and a  $\mu$ App for real-time (<1 ms) intelligent resource allocation. The two RICs operate in concert, sharing information and taking control actions to determine the appropriate spectrum resources to allocate at each site as shown in Figure 1. By using base stations as spectrum sensors, SPARC enables efficient and fine-grained dynamic resource allocation across multiple sites. This approach enhances signal-to-noise ratio (SNR), spectral efficiency, and overall system throughput, making it a robust solution for optimizing resource usage efficiency and network performance.

To address the dual requirements of resource usage efficiency and throughput maximization, SPARC employs multiple Radio Units (RUs) across different sites, leveraging disaggregated cellular architectures such as the O-RAN Split 7.2. This configuration effectively distributes the processing load and enhances local signal strength by permitting the deployment of many relatively simpler/cheaper RUs over a given area. However, the challenge of limited spectrum availability persists, requiring dynamic reallocation to maximize system throughput, especially under variable traffic levels. Efficient spectrum management necessitates sophisticated intelligence capable of operating at very low time granularity to determine and allocate the optimal spectrum parts to specific sites. SPARC introduces several key contributions:

- Multi-timescale RIC Approach: We develop and demonstrate a multi-timescale RIC approach for efficient spectrum management, enabling information sharing and joint optimization using both a near-realtime RIC and a real-time RIC in multi-site scenarios. Our evaluations show a significant enhancement in SNR by up to 7dB.
- Base Station as Spectrum Sensor: We leverage the base station as a spectrum sensor, designing an xApp capable of detecting and localizing interference using object detection techniques. This provides critical information about the physical resource blocks (PRBs) affected by interference.
- **Intelligent Resource Distribution**: Utilizing information from the xApp, we design a  $\mu$ App for intelligent resource distribution in real-time across different RAN sites. This introduces the notion of resource block blanking to optimally redistribute limited spectrum, improving spectral efficiency by up to 15%.
- Comprehensive Evaluations: Through simulations and over-the-air experiments, we validate the benefits of SPARC, observing performance gains in terms of throughput (up to 20%), SNR, and spectral efficiency. These results highlight the effectiveness of the joint capabilities of near-RT RIC and EdgeRIC for multi-site resource sharing.

In summary, SPARC offers a promising solution for enhancing energy efficiency and network performance in next-generation cellular networks through innovative spectrum management and intelligent resource control mechanisms.

#### 2 MOTIVATION AND BACKGROUND

Recent incidents have underscored the critical importance of spectrum awareness in modern communication networks. In one notable instance, a village in Wales with 400 residents experienced daily DSL Internet outages for 18 months due to electrical interference from an old TV [25]. Network operators were baffled until they traced the issue to a single household appliance emitting electrical noise. In another case, a truck driver's GPS jammer disrupted satellite systems at Newark airport [24], interfering with an advanced system designed to improve airport operations. Additionally, concerns have arisen regarding the susceptibility of 5G networks to jamming attacks, which could

lead to denial of service (DoS) in critical applications, with severe impacts on both individuals and infrastructure [23]. These examples illustrate how external interference from stray devices can infiltrate communication bands, causing widespread network disruptions. Such incidents highlight the necessity for robust spectrum awareness to effectively identify and mitigate external interference. Understanding which bands are affected and how to avoid them is crucial for maintaining network integrity. Without this awareness, operators may struggle to pinpoint the source of network failures, increasing the risk of prolonged and widespread outages. Therefore, spectrum awareness is essential for ensuring the reliability and resilience of communication networks.

In this work, our first goal is to leverage the O-RAN architecture to augment a cellular radio network with spectrum sensing capabilities. We utilize base stations as spectrum sensors to collect I/Q samples from the environment and deploy an interference detection and localization module as an xApp on a RAN Intelligent Controller (RIC) to infer the presence and location of interference in the spectrum. The capability for interference detection and localization at teh xApp naturally enables it to provide suggestions blanking out interfered bands for transmission, thus improving the overall signal-to-interference/noise (SINR) ratio and ultimately enhancing system throughput and reducing block error rate (BLER). The concept of Resource Block (RB) blanking immediately leads to valuable use cases, such as resource redistribution across multiple cell sites. Hence our second goal is to support multiple radio units (RUs) operating over the same spectrum by extending RB blanking to optimize resource distribution based on traffic demand in real-time, augmented with situational awareness through spectrum sensing in near-real-time. This approach allows the deployment of multiple RUs over the same spectrum bandwidth, bringing radio transmitters closer to user equipment.

An added advantage of this method addresses the much-debated topic of sustainability. Research by [17] demonstrates that base-station densification can be a viable approach to creating sustainable wireless networks that scale effectively with the number of users. The key insight is that, instead of relying on a single sophisticated base station expending power to reach distant clients, the same task can be accomplished more flexibly and with lower power by using multiple smaller base stations with simpler hardware and reduced signal levels. Further justification for this approach is provided in [16]. They show that the primary contributors to the increased carbon footprint in wireless networks are smartphone batteries impacting the embodied footprint and base stations consuming more energy for last-mile wireless connectivity, both stemming from the lossy wireless medium. The authors show that base-station densification–replacing a single large base station with multiple smaller ones–mitigates this issue, reducing both sources of the increased carbon footprint.

Our system design addresses the desire for sustainability through densification by considering the spectrum sensing and real-time resource allocation under an approach consistent with the O-RAN architecture, where a dense deployment of radio units (RUs), all operating on the same frequency band, are connected to a Distributed Unit (DU). Intelligence is provided by RICs, which play a crucial sensing and control role in the system. The near-RT RIC offers intelligence capabilities through an xApp, which are applications that conduct sensing and optimization of network parameters at a near-real-time granularity (<1s). In our context, we embed spectrum monitoring functionalities within an xApp, enabling the network to detect and reconfigure its parameters in the presence of interference.

At a much smaller time granularity, we utilize EdgeRIC [20], which operates at real-time and hosts  $\mu$ Apps to provide real-time intelligent control. In our case, such control takes the form of deciding how to allocate resources in the presence of interference based on the conditions observed by the xApp. This combined approach allows for effective spectrum management and resource redistribution. Our problem definition is formalized in Figure 2. Case 1 comprises the traditional

:4 Anon.

scenario of a monolithic cellular stack without any spectrum awareness. Case 2 highlights the scenario with spectrum awareness and effective blanking of the interfered Resource Blocks (RBs). Case 3 defines our system, where spectrum resources are distributed among multiple sites, and resource allocation is based on the presence of interference at each physical location. This scenario advocates bringing transmitters closer to user equipment. By incorporating such multi-timescale monitoring and control, we provide a framework for interference avoidance and efficient resource redistribution. To the best of our knowledge, we are the first to approach multi-site management within the O-RAN and RIC framework.

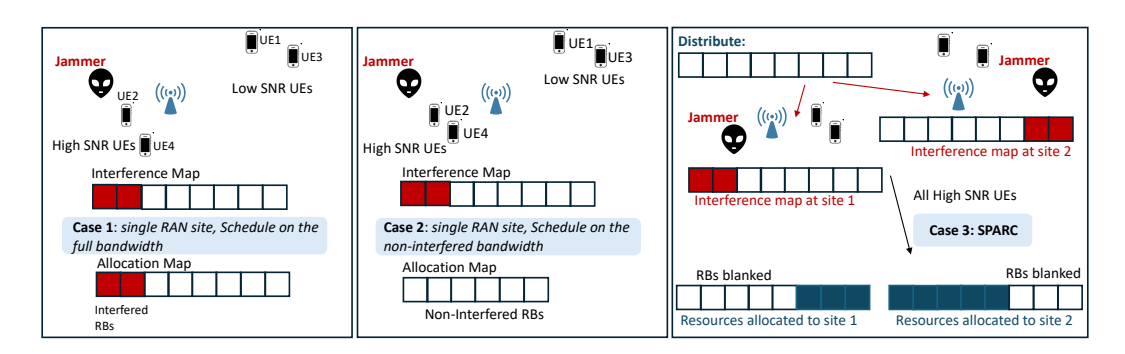


Fig. 2. Problem Definition illustrated

# 2.1 Background on O-RAN

 The cellular network infrastructure is undergoing a shift towards Open Radio Access Networks (Open RAN) [29], promoting diversity and interoperability among RAN vendors and moving away from traditional, monolithic architectures. This shift involves the softwarization and disaggregation of the 5G cellular stack, where the higher layers (Central Unit, CU) are hosted in data centers close to the core and edge servers, and the lower layers (Distributed Units, DUs) handle essential signal processing near the Radio Units (RUs) that transmit the signals. The O-RAN Alliance, comprising industry and academic experts, is focusing on standardizing these networks and defining key use cases [27, 28]. The rise of open-source 5G stacks like Open Air Interface [26] and srsRAN [33], along with the efforts of companies like Mavenir [22], Radisys [30], Nvidia (Aerial Platform, [2]), Microsoft [5], and Intel (FlexRAN, [12]), is driving the development of ORAN-compliant infrastructures, marking a new era in the evolution of radio access networks.

The O-RAN movement is further transforming network architecture by opening interfaces for efficient network metrics collection, facilitating the integration of AI and ML solutions into the network. It introduced standardized, programmable RAN Intelligent Controllers (RICs), currently supporting Near-Real Time (Near-RT RIC) and Non-Real Time (Non-RT RIC) components. The Near-RT RIC supports xApps that use ML algorithms to optimize the RAN within a few milliseconds to a few seconds, leveraging data from the RAN. It also hosts databases and an Internal Messaging Infrastructure (IMI), enabling data routing and connectivity within the RIC through the standardized E2 interface. This interface collects data and allows RIC to communicate control decisions to the RAN. Meanwhile, the Non-RT RIC, part of the Service Management Orchestration (SMO) framework, supports rApps for longer timescale RAN control. Open-source options like OSC RIC [8] and FlexRIC [32] enhance the RIC ecosystem by addressing both non-realtime and near-realtime needs. However, the area of real-time RICs (sub 5ms RAN control) is still emerging, with recent research illuminating their potential within the ORAN framework [11, 13, 14, 20, 21].

 In this work, we explore the potential of leveraging the existing O-RAN architecture to demonstrate the advantages of a multi-timescale monitoring and control approach. We specifically focus on enhancing spatial diversity by extending our system to operate across multiple sites. By employing a collaborative framework between the near Real-Time RIC and the Real-Time RIC, we aim to optimize resource distribution across these sites. This integrated approach allows for more effective management and allocation of resources within the RAN, showcasing the potential of a synchronized multi-RIC system to improve network performance and efficiency.

#### 2.2 Related Work

Spectrum sensing using spectrograms is a widely adopted technique to detect energy levels across various frequency bands [7, 9]. This practice has further evolved with the integration of machine learning (ML) solutions that analyze time-frequency images—spectrograms—generated from detected energy levels at each point [37]. In this work, we leverage an ML-based technique to detect the presence of external interference within our band of interest. We use spectrograms to derive inferences about the spectrum environment and further undergo signal and interference localization in the available spectrum.

While 3GPP standards use reference signals like Sounding Reference Signals (SRS) and Demodulation Reference Signals (DMRS) to estimate channel characteristics on an individual UE basis [1, 18, 38], these do not provide a complete system-wide perspective. In contrast, spectrograms observed at the base station offer a comprehensive view of the spectral environment, enabling the detection of external signals even without active UE traffic. [35] has demonstrated that advanced spectrogram-based detection methods offer deeper insights into spectrum utilization compared to traditional KPI monitoring methods, which analyze communication features like packet error rate (PER), bit error rate (BER), and signal-to-interference-plus-noise ratio (SINR) [36]. In this work, SPARC utilizes spectrograms generated from raw I/Q data collected at each RU to detect and map interference, thereby enhancing network management through optimized frequency allocation.

In the cellular network domain, significant advancements have been made in spectrum sensing to identify and avoid compromised frequency bands. A notable work within the O-RAN framework is ChARM [6], which enhances network management through spectrum awareness. ChARM integrates an additional radio into the base station that processes raw IQ samples to detect interference. Upon identifying suspicious activity, ChARM suggests shifting the entire network's center frequency of operation at the affected site.

Other works in literature targeting spectrum sensing/sharing for optimizing resource utilization include [15], which presents a data-driven spectrum management solution called ProSAS. It offers an intelligent radio resource demand prediction and management scheme for intent-driven spectrum management that minimizes surplus or deficit experienced by RANs. Further, [31] proposes SenseORAN, an enhancement to cellular communications and spectrum sensing facilitated by Open RAN (O-RAN). SenseORAN employs a YOLO-based machine learning framework within the near-RT RIC to detect radar pulses in the CBRS band thereby drastically improving the response time for radar interference management in cellular networks.

However, our work proposes a more nuanced approach by leveraging the spatio-temporal diversity of frequency bands. We are informed by the fact that the impact of interference can vary spatially and temporally, meaning different areas may experience different affected frequency bands at different times. To exploit this effect, we propose deploying multiple transmitters across various locations, each equipped with spectrum sensing capabilities. By doing so, each node can independently identify which part of the spectrum is compromised, specifically which Physical Resource Block (PRB) regions are affected. Our approach involves redistributing the spectrum based on these localized sensing results, allowing each transmitter to operate on the clearest available

246

247

274 275

276

263

265

287

288

289

290

291

292

293 294 frequencies. This method is particularly beneficial in scenarios where an enterprise owns a limited amount of licensed spectrum but aims to maximize utilization across its entire bandwidth. By dynamically adjusting frequency usage according to real-time spectral conditions at various spatial points, our system can enhance overall network performance and efficiency, ensuring optimal use of the available spectrum.

Anon.

#### SYSTEM DESIGN

Figure 3 shows an overview/walkthrough of the main components of our system in context of O-RAN used for multi-site resource sharing. The cellular network must be O-RAN compatible, where the radio units are distributed across different sites. EdgeRIC [20] is responsible for monitoring and control of the DU functionalities, adhering to real time (~1ms) timescales. It communicates with the lower layers of the RAN via the RT-E2 interface. The near-RT RIC operates at a coarser granularity for monitoring (< 1 s) and communicates with the RAN over the E2 interface. We will now summarize the system architecture in the following subsection.

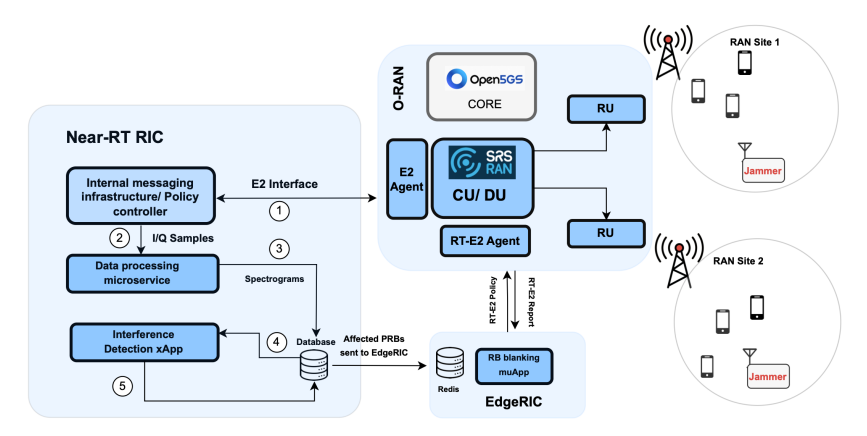


Fig. 3. Overview of System

#### **System Architecture**

We adopt a multi-timescale monitoring and control approach for an optimized system behaviour.

- Spectrum Sensing: A Near Real-time Approach We implement spectrum sensing capabilities for the base station as an xApp, running as a spectrum monitoring, detection and localization microservice in the near-RT RIC. Raw I/Q samples from the RAN sites are collected by the E2 agent through the E2 interface into the RIC for further processing and analysis. An elaborate breakdown of the overall system is as follows:
- (1) After connection establishment between the near-RT RIC and E2 agent which serves as entry point to the RAN, I/Q samples from both RF frontends are forwarded to the policy controller within the near-RT RIC via the E2 interface. These I/Q samples are initially stored in separate buffers to distinguish different RAN sites. For experimental purposes, we periodically collect the last 10 ms segments of I/Q samples from each RAN site which is equivalent to the length of one LTE/5G frame. To reduce round trip time, there can be a trade-off between collecting a full frame of 10 ms or reducing it to 5 ms segments.
- (2) These I/Q samples for the two RAN sites are then forwarded to a data processing microservice which is used to process and convert the raw I/Q samples into spectrograms.

- (3) The data processing microservice then forwards the computed spectrograms to a Redis-based database hosted within the near-RT RIC. This is to ensure that the data is accessible by any xApp that may want to utilize.
- (4) The interference detection/Localization xApp queries the database to get the latest spectrograms for the two RAN sites. These spectrograms give a good picture of the spectrum at the two RAN sites.
- (5) Using the ML model deployed within the xApp, we first detect the presence of interference signal at the two RAN sites using the spectrograms, then we go a step further to determine which Physical Resource Blocks (PRBs) are affected by the interference. These inference results are then forwarded into the database to be used by any other microservice/xApp.
- (6) Finally, the latest information of the affected PRBs is made accessible to EdgeRIC.

# **■** Resource Distribution: A Real-time Approach

The allocation of resources per site is determined every transmission time interval (TTI, 1ms) based on the traffic requirements at each site. EdgeRIC communicates with the MAC layer of the DU to impart control decisions regarding resource allocation by indicating which RBs to blank out for each RU site. Blanked RBs at a site mean those RBs will not be available for use at that site, thereby making them available for use at another site. Essentially, the unblanked RBs are the ones available for use at a particular site or RU.

The communication between EdgeRIC and the RAN occurs over the RT-E2 interface. The RT Report carries information on the RAN state, including pending data and channel quality. The RT E2 policy message consists of the control information, specifically the range of RBs to blank out at a RAN site. The number of RBs to blank depends on the total pending data waiting to be transmitted at each site, which is indirectly a function of the traffic load at the site.

Additionally, situational awareness is crucial for deciding which RBs to allocate to a site. If there is an interfered PRB at a site, it is preferable to avoid transmitting on that PRB. Therefore, we combine the decision on affected PRBs at each site which was derived from the near-RT RIC database, in conjunction with the information regarding each RAN site pending data and channel quality to determine which how many PRBs to allocate to each site.

# 3.2 Interference Detection/Localization xApp

To fully leverage the capabilities and benefits of the O-RAN, particularly the near-RT RIC platform, for multi-site resource sharing, we developed an interference detection and localization algorithm that utilizes spectrograms for both training and inference. This algorithm operates in two steps: first, it processes an image of shape (NxM), where N represents the frequency axis (height) and M represents the time axis (width). Using this image, the model outputs the presence or absence of a jammer or interferring signal, along with the jammer's location dimensions in the spectrum, i.e.,  $J^{NxM} \to \mathcal{F}[f_L, f_H, t_L, t_H], \overline{\mathcal{F}}[F_L, F_H, T_L, T_H], \text{ where } \mathcal{F} \text{ and } \overline{\mathcal{F}} \text{ indicate the presence and absence of a jammer signal, respectively. When a jammer is detected, the model returns a list <math>[f_L, f_H, t_L, t_H],$  where  $f_L$  and  $f_H$  denote the lower and higher frequencies occupied by the jammer as shown in Figure 4a, and  $t_L$  and  $t_H$  represent the time axis dimensions. For our purposes, we focus on the values of  $f_L$  and  $f_H$  to estimate the bandwidth covered by the jammer. Similarly, as illustrated in Figure 4a,  $F_L$  and  $F_H$  indicate the lower and higher frequencies occupied by the LTE/5G signal.

In the first step, we leverage state-of-the-art deep learning algorithms such as Convolutional Neural Networks (CNNs) and You Only Look Once (YOLOV8) [19], using the open-source dataset gotten from over the air experiments in [10] and [34]. We utilize [4], an open-source tool for data annotation, to annotate a few samples in the dataset. To increase the number of samples and variation in the dataset, we employ some data augmentation techniques. A few augmentation

:8 Anon.

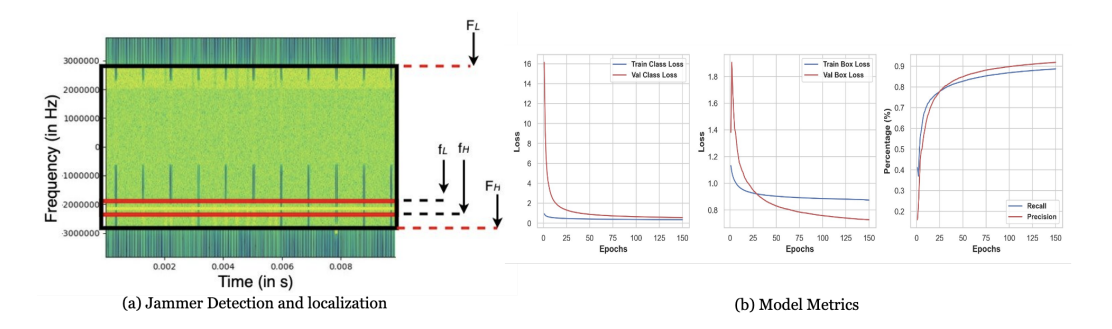


Fig. 4. Object Detection for Interference Detection/Localization and Model Training/Validation Metrics.

techniques we applied on the dataset was to add some gaussian noise to some images, flipping some images horizontally and increasing the brightness on some images to create some level of contrast. All these are done to achieve some level of complexity in the dataset and to ensure our model is able to detect the presence of an interferring signal in any spectrogram under varying conditions.

For the training dataset, we used 2000 images/spectrograms containing information on both the Signal of Interest (SOI) (i.e., the LTE/5G signal) and the jammer in the form of Continuous Wave Interference (CWI) (N.B: Other interference categories can be considered having wider bandwidths and variation in the spectrum). The validation dataset on the other hand consists of 1000 spectrograms.

We leverage YOLOv8l, a pretrained model for detection that has been trained on the popular COCO dataset. This pretrained model consists of 43.7 million parameters. For training on our dataset, we conduct training for 150 epochs with a batch size of 16 and a learning rate of 0.01. These values were observed to provide optimal performance in terms of maximizing accuracy and minimizing loss for detecting the jammer signal, regardless of how narrow the signal bandwidth is in the spectrum. This task is more challenging compared to typical object detection datasets, which feature objects of larger dimensions. Figure 4b shows the metrics derived from the training and validation of our dataset on this model.

For detecting and localizing interference, such as Continuous Wave Interference (CWI), it is crucial to detect every instance of a jammer in the spectrogram while minimizing the probability of false detection to prevent unnecessary resource blanking by the  $\mu$ app. From the metrics plot, we observe that after training for 150 epochs, our model achieves up to 95% precision and 90% recall. Additionally, we focus on the model's ability to accurately detect interference and estimate the bounding box around the interference to determine the correct dimensions of the interference location. Figure 4b also illustrates the box and class losses for both training and validation scenarios, confirming that our model is learning appropriately. Overall, there is still room for optimizing these models to better tailor them for this task and improve the results in these metrics.

After obtaining the values of  $f_L$ ,  $f_H$ ,  $F_L$ , and  $F_H$ , the next step is to estimate which PRBs are affected by the interference signal. This involves utilizing information about the original signal, such as the channel bandwidth, the number of PRBs for the numerology being considered, and the guard bandwidth. Using this information, we first determine the dimensions of the SOI from  $F_L$  and  $F_H$ . Next, we use the guard bands to estimate the actual bandwidth of the signal in terms of the number of PRBs. Once we have this information, we can map the dimensions of the jammer ( $f_L$  and  $f_H$ ) to the corresponding PRBs that it affects.

# 3.3 Multi-site resource distribution on UL Spectrum

3.3.1 Primer on UL scheduling. In LTE, Orthogonal Frequency-Division Multiple Access (OFDMA) is utilized for downlink transmissions. For the uplink transmission, we use Single Carrier Frequency-Division Multiple Access (SC-FDMA), which is essentially equivalent to Discrete Fourier Transform - Orthogonal Frequency-Division Multiplexing (DFT-OFDM). SC-FDMA is chosen for the uplink primarily to reduce the Peak-to-Average Power Ratio (PAPR). OFDMA requires a high energy output, making it less suitable for uplink transmissions. For effective operation, SC-FDMA necessitates contiguous Physical Resource Blocks (PRBs). The uplink scheduling process begins by searching for a contiguous interval of PRBs within the current mask. If no such interval is found, the function returns an empty interval. However, if a contiguous interval is identified, its length is evaluated to ensure it meets SC-FDMA constraints. If the initial interval fails to meet these criteria, the system incrementally extends the interval length one PRB at a time, provided that the total number of PRBs is not exceeded and the next PRB is available. Should extending the interval prove infeasible, the system reduces the interval length until it either complies with SC-FDMA requirements or becomes empty. This dynamic adjustment facilitates energy-efficient and compliant uplink transmissions, albeit restricting us to allocating only contiguous chunks of resources for each site.

3.3.2 Resource blanking. To illustrate the concept of resource blanking, we first consider a scenario without interference. In this case, the weight of a site i ( $w_i$ ) is determined by the sum of the pending UL data buffers at that site. Total demand (demand<sub>i</sub>) at each site i can be calculated as demand<sub>i</sub> =  $\sum_{j \in \text{UEs in site } i}$  pending\_data<sub>j</sub>. Thus,  $w_i$  = demand<sub>i</sub>/ $\sum_i$  demand<sub>i</sub>. The total resources allocated to a site are proportional to  $w_i$  relative to the total available Resource Blocks (RBs). This can be expressed as: rbs\_site<sub>i</sub> = int(round ( $w_i \times n\_prb$ )) where  $n\_prb$  is the total RBs available. Based on the required number of resources, we blank out ( $n\_prb$  - rbs\_site<sub>i</sub>) RBs at each site i

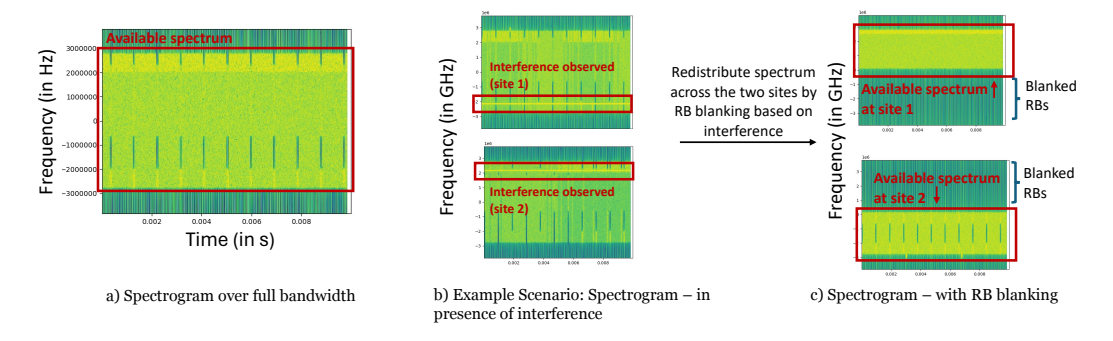


Fig. 5. Spectrogram visualizations: The light green portion indicates available spectrum

Figure 5 elaborates the idea of Resource Block (RB) blanking for effective spectrum management across multiple sites amid interference, illustrated using spectrograms. Figure 5(a) shows the available spectrum over the entire bandwidth, providing a baseline view of the spectrum without any interference. It indicates the full range of frequencies that can be utilized for communication. Figure 5(b) represents the spectrum when interference is present at the sites, marked with a red box is the interference band observed at each site. The presence of interference may affect the available spectrum at the site, thus reducing the effective bandwidth that can be utilized without degradation in signal quality. Figure 5(c) shows the effect of RB blanking to mitigate the interference observed in the previous plot. The top plot indicates the spectrum at site 1 after RB blanking, where the interfered RBs are blanked out, rendering them unavailable at site 1. Consequently, the available

:10 Anon.

spectrum is adjusted to avoid the interfered frequencies. The bottom plot shows the spectrum at site 2, demonstrating that the blanked RBs at site 1 are available for use at site 2. This distribution of spectrum ensures that the overall system efficiency is maintained by utilizing the non-interfered frequencies at each site.

3.3.3 Resource Block Allocation scheme. Here, we elaborate our method to allocate Resource Blocks (RBs) across sites, guided by the interference maps of each site. Algorithm 1 outlines the RB allocation scheme. It takes two primary inputs: the total number of available Physical Resource Blocks  $(n\_prb)$ , and  $sites\_info$ . The latter is a dictionary where each site is the key. This dictionary contains the following attributes for each site: 'weight' indicates the relative demand  $(w_i)$  of the site, 'bad\_rbs' lists the PRBs adversely affected by interference at that site, and 'rbs' stores the required number of RBs at each site  $(rbs\_site_i)$ . Based on the weights, the total available RBs are proportionally distributed among the sites. The algorithm then generates all possible permutations of these allocations to explore different ways of distributing the RBs. For each permutation, it determines the allocation ranges and evaluates the impact of interference on each site by calculating the affected PRBs (Physical Resource Blocks) within these ranges. The permutation that results in the least interference, quantified by the lowest number of affected PRBs ( $bad\_rbs$ ) used for allocation, across all sites, is selected as the optimal allocation.

#### Algorithm 1 Allocation of Resource Blocks (RBs) to Sites

442

443

445

447

449

451

453

455

457

459

490

```
461
           procedure OptimalAllocateRBs(n_prb, sites_info)
                sites_info[site_key]['weight'] = w_i \leftarrow \text{extract weight of each site from sites_info}
463
                sites\_info[site\_key]['rbs'] = rbs\_site_i \leftarrow int(round(w_i \times n\_prb))
         3:
464
                allocations ← all permutations of site keys
         4:
465
                min\ affected \leftarrow \infty
         5:
466
                for each allocation in allocations do
467
                    alloc\_ranges \leftarrow GetRBRanges(allocation, sites\_info)
         7:
468
                    affected \leftarrow CALCULATEAFFECTEDPRBs(alloc\_ranges, sites\_info)
         8:
469
                    if affected < min_affected then
         9:
470
                        min\_affected \leftarrow affected
        10:
471
                        best_allocation \leftarrow {key \rightarrow range for each key in allocation}
        11:
472
                    end if
        12:
473
                end for
        13:
474
                return best_allocation
        14:
475
           end procedure
        15:
476
            function GetRBRanges(allocation, sites_info)
477
                start \leftarrow 0
        17:
478
                for each site_key in allocation do
        18:
479
                    end \leftarrow start + sites\_info[site\_key][`rbs`]
        19.
480
                    sites\_info[site\_key][`alloc\_range`] \leftarrow (start, end - 1)
        20:
481
        21:
                    start \leftarrow end
482
        22:
                end for
483
                return sites info
        23:
484
        24: end function
485
           function CALCULATEAFFECTEDPRBs(alloc_ranges, sites_info)
486
                total\_affected \leftarrow sum affected PRBs in alloc\_ranges
        26:
487
        27:
                return total_affected
488
        28: end function
489
```

 Despite its exhaustive search approach requiring up to n! iterations—where n is the number of sites—the algorithm is computationally efficient. In scenarios devoid of interference, it converges in a single iteration. Computational performance remains robust even as site numbers increase, with the algorithm completing in approximately  $200\mu s$  for five sites and merely  $20\mu s$  for two sites.

#### 3.4 Microbenchmarks

In this section, we present microbenchmarks to validate the benefits of our system. Figure 6 summarizes the performance improvements observed with a context-aware resource block (RB) blanking scheme. Referring back to the cases listed in Figure 2, Case 1 and Case 2 depict a single RAN site scenario, while Case 3 represents our proposed system.

Figure 6(a) shows the Cumulative Distribution Function (CDF) of the Signal-to-Noise and Interference Ratio(SINR) for UE1 (a low SNR UE) and UE2 (a high SNR UE located closer to the transmitter) with and without RB blanking in the presence of interference. The results indicate an SNR improvement by approximately 5dB to 7dB when the affected PRBs are appropriately blanked from the spectrum, thus improving the average signal quality.

Figure 6(b) illustrates the CDF of the total system throughput on the uplink for three different cases: no blanking in a single site (Case 1), blanking applied in a single site (Case 2), and blanking with resource distribution among multiple sites (Case 3). The graph shows that Cases 2 and 3 significantly improve (by  $\sim$ 20%) throughput compared to Case 1, with Case 3 achieving the highest throughput, demonstrating the benefits of our proposed system.

Figure 6(c) depicts the average number of packets dropped per Transmission Time Interval (TTI) over time for the three cases. Case 1 exhibits the highest packet drop rate, while Case 2 shows a substantial reduction in packet errors. Case 3 maintains a consistently low packet drop rate, indicating improved reliability and reduced packet errors by up to 30% compared to the single-site scenario of Case 2.

In summary, the microbenchmarks demonstrate that interference-aware RB blanking for resource distribution across sites can significantly improve SNR, system throughput, and packet error rates, leading to an overall better network performance.

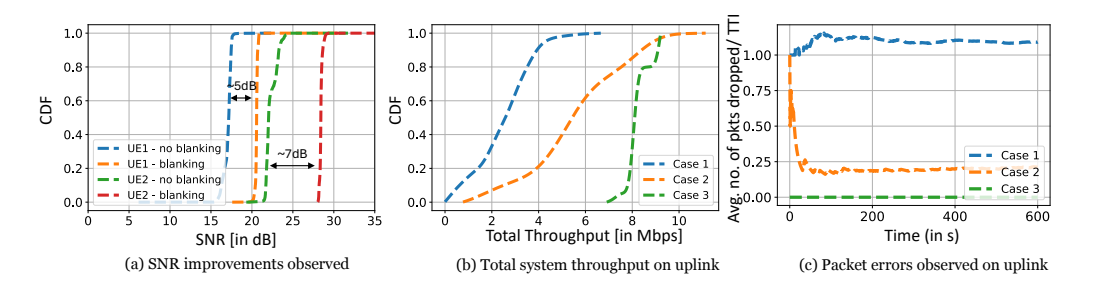


Fig. 6. Microbenchmarks: Interference aware resource distribution across multiple sites (Case 3) does improve network reliability and performance

#### 4 SYSTEM IMPLEMENTATION

For over the air experiments, our setup was designed using the Open AI Cellular (OAIC) platform [3] which is a platform developed for prototyping and testing AI based solutions for next-generation wireless networks. This platform is built on top of the srsRAN [33] codebase version 21.10 hosted on the different desktop computers for the UEs and base stations. Each desktop is equipped with an ubuntu release 20.04 OS and running on an intel core i7-8700 having 6 CPU cores, 16GB RAM,

:12 Anon.



(a) Experiment Setup

 (b) Breakdown of system timing of overall processes

Fig. 7. System Implementation on over the air setup

12 threads and running at a clock speed of 3.2GHz. Each desktop also has USRP B210 Software Defined Radios (SDRs) connected to them. We also have the real-time RIC (EdgeRIC) co-located with the edge distributed unit (DU), a near-RT RIC, and SDR based jammers connected to two different laptop computers running GNU radio. This system setup is shown in Figure 7(a).

The near-RT RIC is hosted on a rack server and has the capacity to serve multiple RANs as shown in Figure 7(a). The server hosting the near-RT RIC is an AMD EPYC™ 7443P with 24 CPU cores, 48 threads, 64GB RAM and a base clock speed of 2.85GHz. It acts as an intelligent controller for the RAN. The near-RT RIC interfaces with the RAN via an E2 interface, allowing it to make decisions and control RAN functions based on real-time data and network conditions. The table in Figure 7(b) presents the overall timing for each step described in section 3.1 explaining our system architecture. This clearly shows that spectrum monitoring occurs on a (<1s) timescale. It can be observed that a chunk of the time here is due to the interference detection and localization step which is due to the fact that the model used for this task has 43.7M parameters. The real-time PRB allocation on the other hand are done within sub-millisecond granularity.

For our experiement which is done in an indoor lab setting, we are operating in the Frequency Division Duplex (FDD) mode and considering the uplink traffic direction from the UEs to the base station operating on the 2.56GHz carrier frequency. We utilize a total of 5MHz bandwidth configuration for analysis which is equivalent to having 25 PRBs. Both base stations and UEs are all stationary for simplicity reasons. For the traffic, we generate different uplink traffic load in the uplink direction for the UEs at different sites using iperf. The UE connected to site one generates 2Mbps of traffic in the uplink direction while the UE connected to the second site generates 4Mbps of traffic in the uplink direction. This is to show the effect of performing resource distribution to different sites based on traffic demand as explained in Section 3.3.

## 4.1 Over the Air System Benchmarks

In Figure 8, we provide some essential observations from the real world setup by trying to answer, *Can we improve network/signal quality with our proposed system?* 

Figure 8(a) illustrates the observed SINR under various scenarios. The "vanilla system w/o IF" (blue curve) represents a setup where both sites fully utilize the entire bandwidth for transmission. In this configuration, SINR is adversely impacted by inter-site interference as a result of the two RAN sites being close, demonstrating lower performance compared to our proposed method (orange curve), which strategically distributes available resources through resource blanking, providing a 10dB gain in SINR. Furthermore, the presence of interference significantly degrades the SINR in the "vanilla system w/ IF" (green curve). In contrast, our proposed system, depicted by the red curve, shows marked improvements in signal quality by effectively blanking out impacted resources at each site, providing a 12dB gain in SINR. While this approach does not match the

 superior performance of the orange curve, as interference still affects other sites, albeit less severely than at the site nearest the jammer, it notably enhances SINR compared to the green curve scenario.

Figure 8(b) presents the packet drop observations, with the trends inversely related to those seen in the SINR plot. This correlation highlights that lower SINR leads to increased packet drops across the network, further underscoring the detrimental impact of poor signal quality on network reliability.

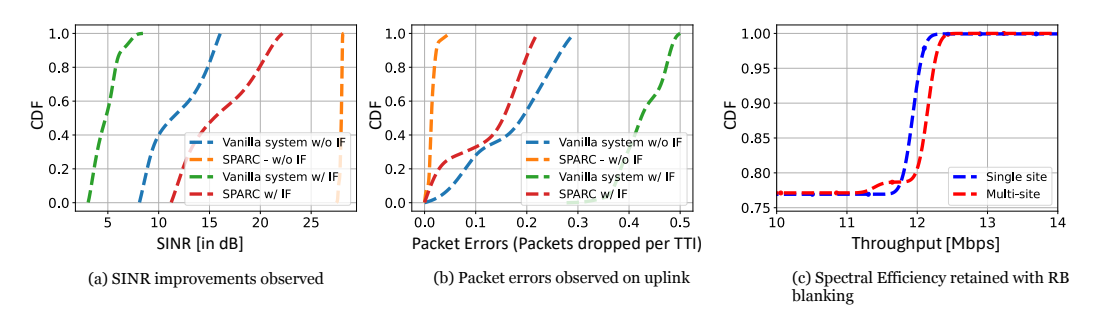


Fig. 8. System Benchmarks: SPARC significantly enhances the network quality

Furthermore, Figure 8(c) addresses the question, *Do we compromise uplink spectral efficiency by resource blanking*? When operating with an equal load on all connected UEs and assuming each UE has a very high uplink SNR, we observe that resource blanking, which redistributes resources across multiple sites, achieves spectral efficiency comparable to that of the traditional single-site scenario. In fact, by increasing the number of transmitters through a multi-site approach, we effectively enhance the uplink SNR for all UEs, thereby potentially increasing spectral efficiency.

# 5 SYSTEM EVALUATIONS

In this section we provide a comprehensive evaluation of our system performance in a wide range of traffic and interference scenarios, trying to specifically answer the following questions, (i) Is demand based real-time resource distribution across multiple sites useful? and (ii) Does spectrum aware resource distribution offer enhanced system behaviour? We specifically compare our proposed system against the following allocation schemes to establish the benefits of **real-time** resource distribution across **multiple sites**:

**Equal Allocation**: A fixed and equal number of resources is reserved for each site.

**Proportional Allocation:** Operating on a coarse granularity timescale (approximately 500ms), this scheme calculates the total bitrate observed at each site over the last 500 slots. Based on this data, it proportionally distributes the spectrum across each site, updating the number of available PRBs every 500 Transmission Time Intervals (TTIs).

**Single RAN site**: We also compare our proposed multi site system performance with a traditional single RAN environment.

In Table 1, we detail various traffic scenarios to assess our system, which comprises four UEs connected to two RUs within the cellular network. Specifically, UE1 and UE2 are connected to RU1, while UE3 and UE4 connect to RU2. It is presumed that all UEs are proximate to their transmitters, thereby benefitting from strong uplink channels. Scenarios 1 through 5 (Sc 1-5) employ iperf as the traffic generator. In contrast, Scenario 6 (Sc 6) utilizes a custom traffic generator designed to simulate different traffic profiles. For instance, the Enhanced Mobile Broadband (eMBB) and Extended Reality (XR) scenarios involve periodic traffic, where packets are generated at fixed intervals—akin to video

 :14

frame rates. The eMBB scenario is configured for a traffic load of 3 Mbps, while the XR scenario supports 5 Mbps. Additionally, the Ultra-Reliable Low-Latency Communications (URLLC) traffic flow is characterized by bursty patterns, with random bursts of 3-5 MB occurring sporadically.

Anon.

Table 1. Summary of all scenarios

Scenarios	Traffic profile for the connected UEs
Static Traffic	
Sc 1	iperf - UE1: 3Mbps, UE2: 8Mbps, UE3: 2Mbps, UE4: 9Mbps
Sc 2	iperf - UE1: 7Mbps, UE2: 1Mbps, UE3: 7Mbps, UE4: 1Mbps
Sc 3	iperf - UE1: 7Mbps, UE2: 7Mbps, UE3: 1Mbps, UE4: 1Mbps
Sc 4	iperf - UE1: 3Mbps, UE2: 6Mbps, UE3: 0.01Mbps, UE4: 0.01Mbps
Dynamic Traffic	
Sc 5	iperf traffic: offered load randomly changes b/w 2-9 Mbps every 1s for all UEs
Sc 6	Custom traffic: UE1: embb, UE2: urllc, UE3: XR, UE4: urllc

# 5.1 Impact of real-time demand-based multi site resource distribution

In this subsection, we present evaluations (Figure 9) to address our first research question: Is demand-based, real-time resource distribution across multiple sites beneficial?

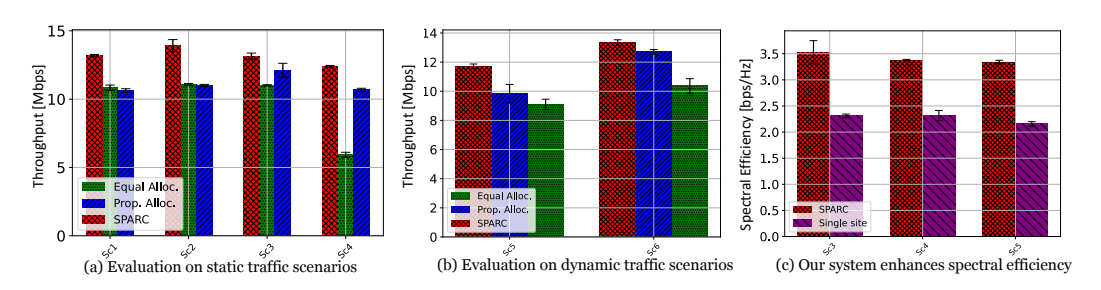


Fig. 9. Real-time resource distribution across multiple sites via SPARC enhances the total system throughput

Figure 9(a) illustrates scenarios with static traffic profiles, where the traffic offered to each UE remains constant throughout our experiments. Scenarios 1 and 2 (Sc1 and Sc2) involve cases where the total traffic demand at both sites is equivalent. In these scenarios, we observe that performance under the Equal Allocation (Equal Alloc.) and Proportional Allocation (Prop. Alloc.) schemes is comparable. However, we observe that the total amount of data pending for transmission can vary significantly at any given moment. By adopting a real-time approach that adjusts resource distribution based on the instantaneous total data pending at each site, we can surpass the performance of both the Equal and Proportional Alloc. schemes. Similar patterns are evident in Scenarios 3 and 4 (Sc3 and Sc4), where the traffic demand differs between the sites—site1 requires more resources than site2. In these cases, Equal alloc results in poorer performance, while PF moderately improves resource allocation by adjusting to the traffic at a coarser timescale. Nonetheless, our approach, which makes instantaneous resource distribution decisions, consistently achieves superior throughput, thereby validating its effectiveness in enhancing system performance. SPARC is able to support at least 20% higher system throughput.

Figure 9(b) displays results for scenarios (Sc 5 and Sc 6) where traffic flow varies among the UEs throughout the duration of our experiments. These scenarios further confirm that real-time

 decision-making enhances system performance, providing optimal outcomes even under fluctuating traffic conditions.

In Figure 9(c), we explore how our multi-site system stacks up against traditional single-site configurations. By strategically positioning transmitters or RUs closer and more densely around UEs, we significantly improve the uplink SNR. This setup increases the achievable bitrate and the Modulation and Coding Scheme (MCS), thus substantially boosting overall system throughput.

# 5.2 Impact of interference-aware demand-based multi site resource distribution

In this subsection, we provide evaluations to address our second question: Does spectrum-aware resource distribution enhance system behavior? Given the critical role of spectrum awareness in identifying external interference—such as jammers that can severely disrupt operations—we present our results in Figure 10, which illustrates how our system performs under various traffic profiles in the presence of interference.

We introduce frequency-hopping interferers in our system, specifically single-tone jammers that transmit randomly across various frequencies within our spectrum of interest. Leveraging the interference detection and localization xApp, which operates within the near-RT RIC, we can accurately detect these interfering frequencies. This detection allows us to strategically avoid these frequencies at each site. EdgeRIC is then updated about the interfered or compromised PRBs at each site, enabling it to judiciously select the parts of the spectrum to allocate per site.

Figure 10(a) highlights the throughput benefits of our proposed multi-site system in the presence of interference across various traffic profiles. SPARC support at least 25% higher throughput in all scenarios. Figure 10(b) corroborates these benefits by showing the improved uplink average SINR achieved when the system efficiently avoids the compromised frequencies. Finally, Figure 10(c) demonstrates how our system significantly reduces packet drops by steering clear of the bad channel RBs, thereby potentially lowering overall latency by eliminating the need for retransmissions. SPARC is able to offer near to zero percent packet drops.

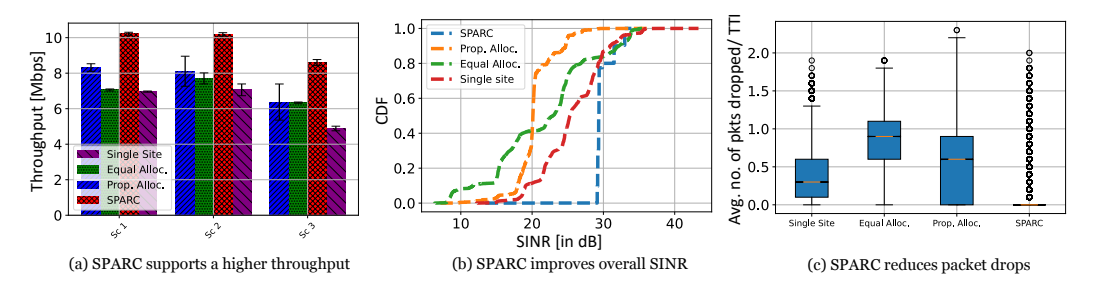


Fig. 10. Summary of system benefits realized by SPARC under interference

#### 6 CONCLUSION

In this paper, we have presented a comprehensive evaluation of a multi-site cellular network system that incorporates near real-time spectrum monitoring and real-time spectrum-aware resource distribution strategies. Through experimentation and analysis, we have effectively answered two pivotal questions that underscore the necessity and benefits of our approach.

Firstly, we demonstrated that demand-based, real-time resource distribution significantly enhances system throughput. Our evaluations revealed that by dynamically adjusting resource allocations based on instantaneous traffic demands and data pending at multiple sites, we could achieve superior performance compared to traditional single site systems.

:16 Anon.

Secondly, the introduction of spectrum-aware resource distribution has proven to be a critical advancement in combating external interferences such as jammers. By employing sophisticated detection capabilities within the near-RT RIC and effectively managing spectrum allocation through EdgeRIC, our system maintained high throughput and improved SINR despite the presence of frequency-hopping interferers. This capability reduced packet drops and the associated need for retransmissions, thereby demonstrating potential for enhancing the overall network reliability and latency.

**Ethical concerns:** This work does not raise any ethical issues.

#### REFERENCES

736

737 738

739

740

741

743

744 745

747

749

750

751

753

755

757

758

759

760

761

762

763

764

765

766

767

768

769

770

771

772

773

774

775

776

777

778

779

780

781

782

783 784

- [1] 2014. Review of channel quality indicator estimation schemes for multi-user MIMO in 3GPP LTE/LTE-A systems. KSII Trans. Internet Inf. Syst. 8, 6 (June 2014), 1848–1868.
- [2] 2023. Nvidia Aerial. (2023). https://developer.nvidia.com/aerial
- [3] 2023. Open AI Cellular. (2023). https://github.com/openaicellular
- [4] 2024. Open Data Annotation Platform. https://www.cvat.ai/. (2024).
- [5] Paramvir Bahl, Matthew Balkwill, Xenofon Foukas, Anuj Kalia, Daehyeok Kim, Manikanta Kotaru, Zhihua Lai, Sanjeev Mehrotra, Bozidar Radunovic, Stefan Saroiu, Connor Settle, Ankit Verma, Alec Wolman, Francis Y. Yan, and Yongguang Zhang. 2023. Accelerating Open RAN Research Through an Enterprise-scale 5G Testbed. Association for Computing Machinery, New York, NY, USA. https://doi.org/10.1145/3570361.3615745
- [6] Luca Baldesi, Francesco Restuccia, and Tommaso Melodia. 2022. ChARM: NextG Spectrum Sharing Through Data-Driven Real-Time O-RAN Dynamic Control. In IEEE INFOCOM 2022 - IEEE Conference on Computer Communications. IEEE Press, 240–249. https://doi.org/10.1109/INFOCOM48880.2022.9796985
- [7] Richard Bell, Kyle Watson, Tianyi Hu, Isamu Poy, fred harris, and Dinesh Bharadia. 2023. Searchlight: An accurate, sensitive, and fast radio frequency energy detection system. 397–404. https://doi.org/10.1109/MILCOM58377.2023. 10356230
- [8] Fransiscus Asisi Bimo, Ferlinda Feliana, Shu-Hua Liao, Chih-Wei Lin, David F. Kinsey, James Li, Rittwik Jana, Richard Wright, and Ray-Guang Cheng. 2022. OSC Community Lab: The Integration Test Bed for O-RAN Software Community. (2022). arXiv:cs.NI/2208.14885
- [9] Lianning Cai, Kaitian Cao, Yongpeng Wu, and Zhou Yuan. 2022. Spectrum Sensing Based on Spectrogram-Aware CNN for Cognitive Radio Network. IEEE Wireless Communications Letters 11 (10 2022), 1–1. https://doi.org/10.1109/ LWC.2022.3194735
- [10] Azuka Chiejina, Brian Kim, Kaushik Chowhdury, and Vijay K Shah. 2024. System-level Analysis of Adversarial Attacks and Defenses on Intelligence in O-RAN based Cellular Networks. In Proceedings of the 17th ACM Conference on Security and Privacy in Wireless and Mobile Networks. 237–247.
- [11] Salvatore D'Oro, Michele Polese, Leonardo Bonati, Hai Cheng, and Tommaso Melodia. 2022. dApps: Distributed Applications for Real-Time Inference and Control in O-RAN. *IEEE Communications Magazine* 60, 11 (2022), 52–58. https://doi.org/10.1109/MCOM.002.2200079
- [12] Xenofon Foukas, Navid Nikaein, Mohamed M. Kassem, Mahesh K. Marina, and Kimon Kontovasilis. 2016. FlexRAN: A Flexible and Programmable Platform for Software-Defined Radio Access Networks. In Proceedings of the 12th International on Conference on Emerging Networking Experiments and Technologies (CoNEXT '16). Association for Computing Machinery, New York, NY, USA, 427–441. https://doi.org/10.1145/2999572.2999599
- [13] Xenofon Foukas, Bozidar Radunovic, Matthew Balkwill, and Zhihua Lai. 2023. Taking 5G RAN Analytics and Control to a New Level (ACM MobiCom '23). Association for Computing Machinery, New York, NY, USA, Article 1, 16 pages. https://doi.org/10.1145/3570361.3592493
- [14] Xenofon Foukas, Bozidar Radunovic, Matthew Balkwill, Zhihua Lai, and Connor Settle. 2023. Programmable RAN Platform for Flexible Real-Time Control and Telemetry. Association for Computing Machinery, New York, NY, USA. https://doi.org/10.1145/3570361.3614065
- [15] Sneihil Gopal, David Griffith, Richard A Rouil, and Chunmei Liu. 2024. ProSAS: An O-RAN Approach to Spectrum Sharing between NR and LTE. arXiv preprint arXiv:2404.09110 (2024).
- [16] Agrim Gupta, Adel Heidari, Jiaming Jin, and Dinesh Bharadia. 2024. Densify & Conquer: Densified, smaller base-stations can conquer the increasing carbon footprint problem in nextG wireless. (2024). arXiv:cs.NI/2403.13611
- [17] Agrim Gupta, Ish Jain, and Dinesh Bharadia. 2022. Multiple smaller base stations are greener than a single powerful one: Densification of wireless cellular networks. In 1st Workshop on Sustainable Computer Systems Design and Implementation (HotCarbon).

788

789

790

791

792

793

794

796

798

800

801

802

804

806

807

808

809

810

811

812

813

814

815

816

817

818

819

820

821

822

823

824

- [18] Xiaolin Hou and Hidetoshi Kayama. 2011. Demodulation reference signal design and channel estimation for LTE-Advanced
   uplink. INTECH Open Access Publisher.
  - [19] Jacob Solawetz and Francesco. 2024. What is YOLOv8? The Ultimate Guide. [2024]. https://blog.roboflow.com/whats-new-in-yolov8/. (2024).
  - [20] Woo-Hyun Ko, Ushasi Ghosh, Ujwal Dinesha, Raini Wu, Srinivas Shakkottai, and Dinesh Bharadia. 2024. EdgeRIC: Empowering Real-time Intelligent Optimization and Control in NextG Cellular Networks. In 21st USENIX Symposium on Networked Systems Design and Implementation (NSDI 24). USENIX Association, Santa Clara, CA, 1315–1330. https://www.usenix.org/conference/nsdi24/presentation/ko
  - [21] Chang Liu, Gopalasingham Aravinthan, Ahan Kak, and Nakjung Choi. 2023. TinyRIC: Supercharging O-RAN Base Stations with Real-time Control. Association for Computing Machinery, New York, NY, USA. https://doi.org/10.1145/ 3570361.3615743
  - [22] Mavenir, Inc. 2022. Mavenir, Inc. https://www.mavenir.com/. (2022).
  - [23] Jorge Navarro-Ortiz, Pablo Romero-Diaz, Sandra Sendra, Pablo Ameigeiras, Juan J. Ramos-Munoz, and Juan M. Lopez-Soler. 2020. A Survey on 5G Usage Scenarios and Traffic Models. IEEE Communications Surveys Tutorials 22, 2 (2020), 905–929. https://doi.org/10.1109/COMST.2020.2971781
  - [24] News Article 2013. Intentional jamming by truck driver at new york airport. https://www.cnet.com/culture/truck-driver-has-gps-jammer-accidentally-jams-newark-airport/. (2013).
  - [25] News Article 2020. old tv set interferes with connectivity:. https://arstechnica.com/information-technology/2020/09/old-tv-set-interfered-with-villages-dsl-internet-each-day-for-18-months/. (2020).
  - [26] Navid Nikaein, Mahesh K. Marina, Saravana Manickam, Alex Dawson, Raymond Knopp, and Christian Bonnet. 2014. OpenAirInterface: A Flexible Platform for 5G Research. SIGCOMM Comput. Commun. Rev. 44, 5 (oct 2014), 33–38. https://doi.org/10.1145/2677046.2677053
  - [27] ORAN Alliance Feb, 2019. O-RAN use cases and deployment scenarios. Tech Republic.. (Feb, 2019).
  - [28] ORAN Alliance March, 2019. O-RAN working group 2: AI/ML workflow description and requirements. Tech Republic.. (March, 2019).
  - [29] Michele Polese, Leonardo Bonati, Salvatore D'Oro, Stefano Basagni, and Tommaso Melodia. 2023. Understanding O-RAN: Architecture, Interfaces, Algorithms, Security, and Research Challenges. *Commun. Surveys Tuts.* 25, 2 (apr 2023), 1376–1411. https://doi.org/10.1109/COMST.2023.3239220
  - [30] Radisys, Inc. 2022. Radisys, Inc. https://www.radisys.com/. (2022).
  - [31] Guillem Reus-Muns, Pratheek S Upadhyaya, Utku Demir, Nathan Stephenson, Nasim Soltani, Vijay K Shah, and Kaushik R Chowdhury. 2023. Senseoran: O-RAN based radar detection in the cbrs band. *IEEE Journal on Selected Areas in Communications* (2023).
  - [32] Robert Schmidt, Mikel Irazabal, and Navid Nikaein. 2021. FlexRIC: an SDK for next-generation SD-RANs. In Proceedings of the 17th International Conference on Emerging Networking Experiments and Technologies (CoNEXT '21). Association for Computing Machinery, New York, NY, USA, 411–425. https://doi.org/10.1145/3485983.3494870
  - [33] srsRAN, Inc. 2023. srsRAN, Inc. https://www.srslte.com/. (2023).
  - [34] Nathan H. Stephenson, Azuka J. Chiejina, Nathaniel B. Kabigting, and Vijay K. Shah. 2023. Demonstration of Closed Loop AI-Driven RAN Controllers Using O-RAN SDR Testbed. In MILCOM 2023 - 2023 IEEE Military Communications Conference (MILCOM). 241–242. https://doi.org/10.1109/MILCOM58377.2023.10356330
  - [35] Matteo Varotto, Stefan Valentin, and Stefano Tomasin. 2024. Detecting 5G Signal Jammers Using Spectrograms with Supervised and Unsupervised Learning. (2024). arXiv:2405.10331
  - [36] Yujia Zhang, Guanlin Chen, Wenyong Weng, and Zebing Wang. 2010. An overview of wireless intrusion prevention systems. In 2010 Second International Conference on Communication Systems, Networks and Applications, Vol. 1. 147–150. https://doi.org/10.1109/ICCSNA.2010.5588671
  - [37] Yixuan Zhang and Zhongqiang Luo. 2023. A Review of Research on Spectrum Sensing Based on Deep Learning. Electronics 12, 21 (2023). https://doi.org/10.3390/electronics12214514
  - [38] Jim Zyren and Wes McCoy. 2007. Overview of the 3GPP long term evolution physical layer. Freescale Semiconductor, Inc., white paper 7 (2007), 2–22.